Temperature extremes of 2022 reduced carbon uptake by forests in Europe

Wouter Peters (wouter.peters@wur.nl)
Wageningen University and Research Centre https://orcid.org/0000-0001-8166-2070

Auke van der Woude
Groningen University

Ingrid Luijkx
Wageningen University https://orcid.org/0000-0002-3990-6737

Emilie Joetzjer
Université de Lorraine

Sébastien Lafont
Institut National de la Recherche Agronomique

Benjamin Loubet
UMR ECOSYS, AgroParisTech, INRAE, Université Paris-Saclay

Pedro-Henrique Herig-Coimbra
Université Paris-Saclay

Denis Loustau
ISPA, Bordeaux Sciences Agro, INRAE

Gerbrand Koren
Copernicus Institute of Sustainable Development, Utrecht University https://orcid.org/0000-0002-2275-0713

Philippe Ciais
Laboratoire des Sciences du Climat et de l'Environnement https://orcid.org/0000-0001-8560-4943

Michel Ramonet
LSCE Paris

Yidi Xu
Tsinghua University

Ana Bastos
Max Planck Institute for Biogeochemistry https://orcid.org/0000-0002-7368-7806

Stephen Sitch
University of Exeter https://orcid.org/0000-0003-1821-8561

Tobias Kneuer
Deutscher Wetterdienst

Dagmar Kubistin
Deutscher Wetterdienst https://orcid.org/0000-0002-5467-9309

Remco De Kok
Wageningen University
Santiago Botía
Max Planck Institute for Biogeochemistry

Article

Keywords:

Posted Date: May 2nd, 2023

DOI: https://doi.org/10.21203/rs.3.rs-2841861/v1

Additional Declarations: There is **NO** Competing Interest.

Version of Record: A version of this preprint was published at Nature Communications on October 6th, 2023. See the published version at https://doi.org/10.1038/s41467-023-41851-0.

Temperature extremes of 2022 reduced carbon uptake by forests in Europe

Auke M. van der Woude[1,2,+], Wouter Peters[2,1,+,*], Emilie Joetzjer[3], Sébastien Lafont[4], Benjamin Loubet[4], Denis Loustau[4], Pedro-Henrique Herig-Coimbra[4], Gerbrand Koren[5], Philippe Ciais[6], Michel Ramonet[6], Yidi Xu[6], Ana Bastos[7], Santiago Botía[7], Stephen Sitch[8], Tobias Kneuer[10], Dagmar Kubistin[10], Remco de Kok[2,9], and Ingrid T. Luijkx[2]

[1]University of Groningen, Centre for Isotope Research, Groningen, 8481 NG, The Netherlands
[2]Wageningen University, Meteorology & Air Quality Dept, Wageningen, 6700 AA, The Netherlands
[4]Functional Ecology and Environmental Physics, Ephyse, INRA, Villenave d'Ornon, France
[5]Copernicus Institute of Sustainable Development, Utrecht University, Utrecht, the Netherlands
[6]UMR CEA-CNRS-UVSQ, Laboratoire des Sciences du Climat et de l'Environnement, Gif sur Yvette, France
[7]Max Planck Institute for Biogeochemistry, Jena, Germany
[8]Faculty of Environment, Science and Economy, University of Exeter, Exeter, UK
[9]ICOS ERIC, Carbon Portal, Geocentrum II, Sölvegatan 12, SE-22362 Lund, Sweden
[3]Université de Lorraine, AgroParisTech, INRAE, UMR Silva, 54000 Nancy, France
[10]Deutscher Wetterdienst, Hohenpeissenberg Meteorological Observatory, Hohenpeissenberg, Germany
[*]corresponding author: Wouter.Peters@wur.nl
[+]these authors contributed equally to this work

ABSTRACT

The year 2022 saw record breaking temperatures in Europe during both summer and fall. Close to 30% of the European continent was under severe summer drought with a similarly large area affected (3.0 million km^2) as during the recent 2018 drought, but now located in central and southeastern Europe. Multiple sets of observations suggest a reduction of net ecosystem carbon exchange in summer (57-62 TgC) over this area, and specific sites in France even showed a widespread summertime carbon *release* by forests, as well as wildfires. A warm fall with prolonged carbon uptake offered only partial compensation (up to 32%) for the carbon uptake lost due to drought. This severity of this second drought event in 5 years suggests these impacts to no longer be exceptional, and important to factor into Europe's developing plans for net-zero greenhouse gas emissions that rely on carbon sequestration by forests.

Introduction

The year 2022 marked another year of temperature extremes in Europe. In summer, record temperatures over 40 °C in mid-latitude countries such as France, the UK, and the Netherlands[1], and water temperatures over 30 °C in the Mediterranean Sea[2] occurred. Subsequent autumn temperatures were also elevated, with mean temperature for the months of October, November and December exceeding the long-term mean by several degrees, especially in southern Europe[3]. In western Europe this extreme summer heat is often associated with so-called blocking events when stationary Rossby wave trains across the northern hemisphere keep high pressure areas in place over the continent, diverging moisture inflow from the Atlantic ocean north- and southwards relative to its normal westerly path[4–6]. This "wave-7" blocking pattern occurs more frequently during positive phases of the North Atlantic Oscillation (NAO[7]), and is suggested to occur more frequently with increasing climate warming[4,8]. The intense droughts of 2003, 2015, 2018, and 2022 each played out under such conditions[9–12], with several studies confirming an important role for human-made climate warming[13,14]. Although painted as exceptional climate conditions in the media, these heat and rainfall patterns have a much reduced return time of 10-15 years under current global warming[15–17], and will be part of the "new normal" of the decades to come.

The 2022 large-scale drought and temperature anomalies we report here thus fit a reported shift of summer climate extremes[15]. Accumulating drought experience and better national heat plans in Spain, Portugal France, Germany, Belgium, and the Netherlands limited the worst impacts —such as the 70,000 excess deaths in 2003[18]— but water shortages, shipping disruptions, wildfires, crop yield loss, and forest degradation were nevertheless widespread once again[2]. From the perspective of forestry, fire management, agriculture, biodiversity, and carbon sequestration in Europe it is of great importance to understand the impact on carbon exchange by vegetation and soils in Europe. Especially sequestration is gaining recent attention, as

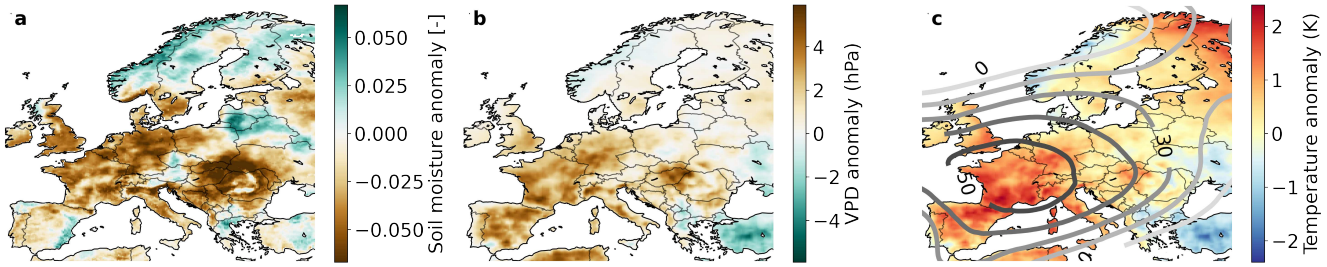

Figure 1. Overview of the European drought in 2022. Soil moisture (a) and vapour pressure deficit (VPD) anomalies (b), representing soil and atmospheric drought respectively. Panel c shows temperature anomalies, indicating elevated temperatures over large parts of Europe. Geopotential height (GPH) anomalies (500hPa, in metres), relative to 1980-2022, for MJJA 2022 are indicated with contours. Soil moisture is taken from ERA5-Land[21], temperature, VPD and GPH are taken from ERA5[22].

the vast majority of countries included a large potential for carbon sequestration by the forestry sector in their Nationally Determined Contributions to the Paris Agreement. This study investigates the impact of the 2022 summer drought on carbon exchange between European forests and the atmosphere, from a diverse set of ground- and space- based monitoring platforms. By placing the 2022 event in context of previous strong summer droughts[19,20], we try to answer the question whether the carbon cycle impact of the 2022 extreme drought event was an exceptional, or exemplary, situation for upcoming drought impacts on forests.

Anatomy of the summer drought

In 2022, the center of anomalously high pressure was centered over France (see Fig. 1) much like during the record heat wave of 2003[19] and large-scale conditions resemble the diagnosed state from that event. Like in 2003, high sea-surface temperatures in the Mediterranean Sea and low winter/spring precipitation in southern Europe[23] contributed to low soil moisture levels in early summer (See Fig. 1 and supplementary material S1), likely triggering land-surface feedbacks known to exacerbate summer heat and drought[24–27]. This contrasts the more atypical 2018 drought event over northern Europe, which occurred while the NAO index was anomalously high (+1.65 from May 2018 to September 2018) pushing the stationary high pressure center northwards towards Scandinavia[4,20]. Fig. 1 shows the geopotential height anomalies in 2022 and Fig. 2 shows the areas under severe drought (3-month standardized precipitation and evaporation index (SPEI) <-1.2) in July 2018 (blue areas, 2.7 million km^2) and in July 2022 (yellow and red areas, 3.0 million km^2), with the blue/yellow hatched area marking the region where both droughts hit (0.8 million km^2) (see also Supplementary Section A). We distinguish (in red) a secondary center of severe drought impact in June-July-August (JJA) 2022 which was located over in the Eastern part of Europe (Croatia, Bulgaria, Romania, and Slovenia), away from the high-pressure anomaly over France (Fig. 1). The temperate land-climate (Köppen class D) of this area differs from the sea-climate (Köppen class C) between the Atlantic and Mediterranean sea, and it also has a distinct land-use with extensive broadleaf and beech forests.

In contrast to the 2018 drought, which was preceded by a wet winter and a warm and sunny spring[20], the 2022 drought developed from already low soil moisture (SM) levels since winter (also see[9]). And rather than a warm spring, the 2022 summer drought was followed by anomalously warm conditions and persisting low soil moisture in autumn. Although a clear soil moisture anomaly is seen over Europe from February onwards (Fig. 1, also see Fig. S1 and Supplementary Section B), this anomaly is not outside the 2σ range for the vast majority of the drought-affected area. However, another relevant driver of heat wave impacts in summer is the combination of atmospheric excess heat and low humidity, as seen through the vapor pressure deficit (VPD). Using the ERA5 reanalysis[22] to spatially integrate over the three affected areas shown in Figure 1, we show that JJA-2022 had the highest VPD of any of the last 20 years in 45/51/15% of the area under the central/south/east contour respectively, with JJA-2018 close behind (also see Supplementary Fig. S3). We next report the widespread impacts of these effects on the carbon balance of the atmosphere and forests across Europe.

Net carbon exchange impacts

The network of the Integrated Carbon Observing System (ICOS[29]) recorded positive anomalies in atmospheric CO_2 mole fractions across southern- and western Europe in near real-time, summarized in Fig. 3 (see also Supplementary Section C). Higher than average (2019-2021) mole fractions (see Supplementary material C) across central Europe could indicate either reduced Net Ecosystem Exchange (NEE), or a change in atmospheric circulation with advection of more northerly and CO_2-enriched air masses. We find, based on both observation- and model-based analyses, that the reduction in NEE was the dominant impact in July and August ($\pm$75% of the CO_2 signal, see Supplementary Table D), with sites in southern France showing >2.5ppm excess CO_2 in JJA, relative to 2019-2021 (see Supplementary Section C).

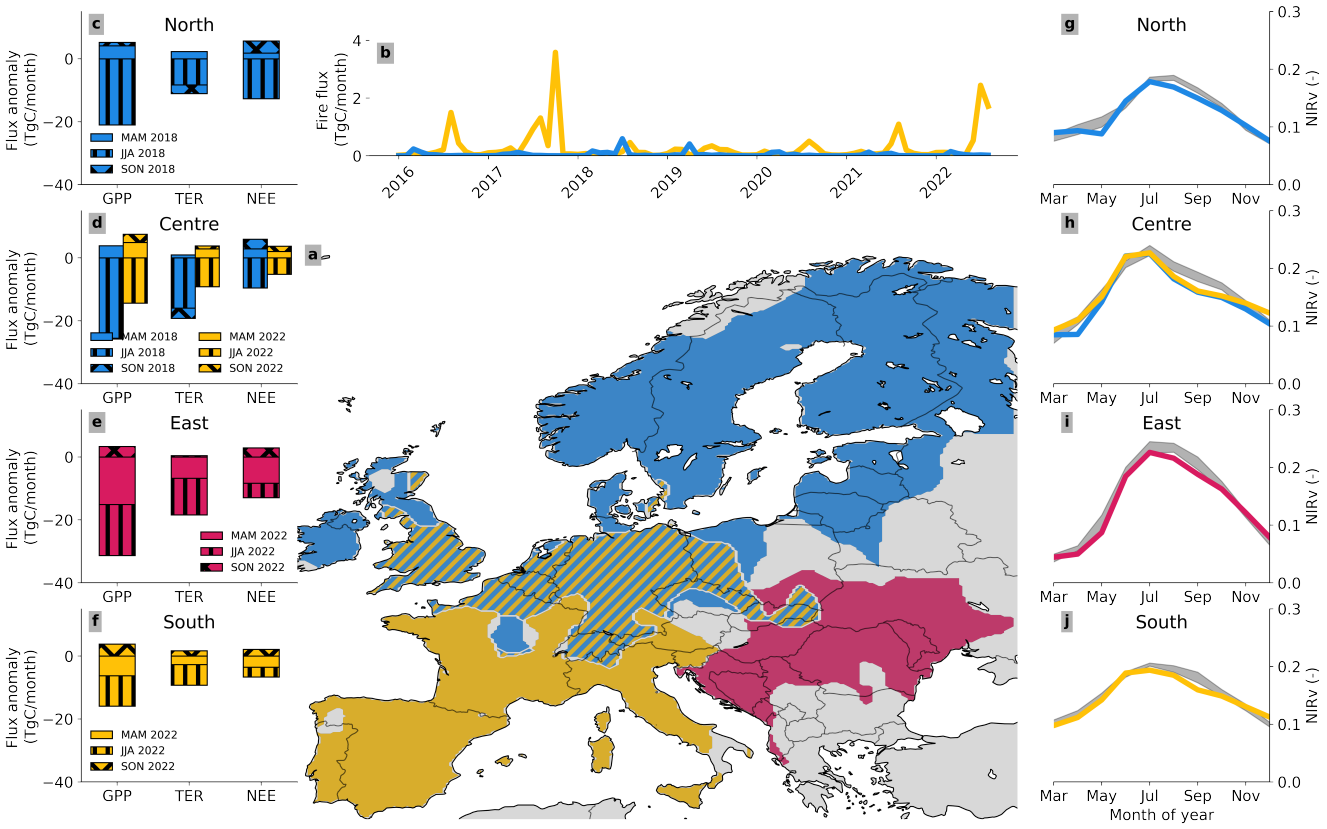

Figure 2. Overview of the carbon impact of the European droughts of 2022 and 2018. (a) The different regions struck by the droughts (See Supplementary Section A) of 2018 ("North" in blue), 2022 ("South" in yellow, "East" in red), or both year ("Centre" in blue/yellow hatched). Note that the East region is far away from the centre of the 2022 geopotential height anomaly 1. (b) Fire fluxes, taken from GFAS[28] over the South (blue) and North (red) regions. (c-f) Biosphere flux anomalies per region relative to 2016-2021 for MAM (clear), JJA (vertical hatching), and SON (crossed hatching), as calculated by the biosphere model SiB4 (see Supplementary Section G). (g-j) Monthly mean MODIS NIRv signal (see Supplementary Section F) per region for drought years, compared with the climatology between 2016-2022. Colours in panels c-j refer to the regions of the same colour in panel a, where panels d and h correspond to the central region, with yellow and blue and representing 2022 and 2018, respectively.

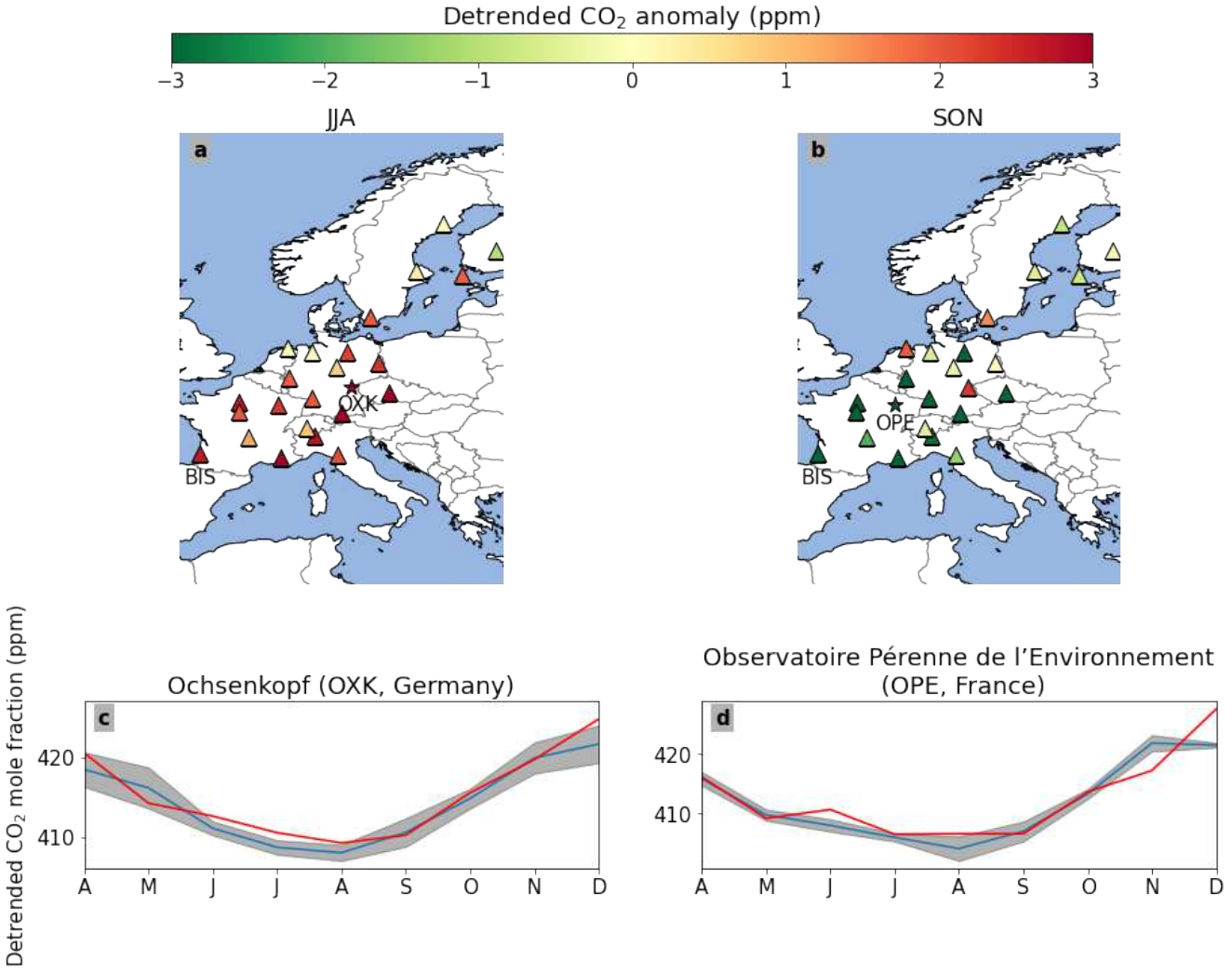

Figure 3. The carbon impact of the 2022 drought from an atmospheric perspective: atmospheric CO_2 anomalies due to flux anomalies for JJA (a) and SON (b) 2022 (see Supplementary Section C), relative to 2019-2021, together with CO_2 monthly mean values in 2022 (red) and 2019-2021 (grey, with one standard deviation in blue) at the representative sites Ochsenkopf (OXK, C) and Observatoire pérenne de l'environnement (OPE, d).

Biomass burning contributed substantially to higher CO_2 mole fractions only at site Biscarosse, near the largest fires in the region of Les Landes, France, as evidenced by simultaneous increases in carbon monoxide (CO) mole fractions with 1-day averaged values exceeding 1000 ppb in early July (Supplementary Fig. S4). Below, we show a more detailed analysis of the impacts of fires. Overall, the broader spatial pattern offered by the ICOS network confirms the more southerly center of drought impact compared to 2018, with a larger integrated atmospheric CO_2 summer anomaly.

A quantification of the impact on net ecosystem exchange during JJA suggests a reduction of carbon uptake of 57-62 TgC, relative to 2019-2021, over the affected areas shown in Figure 1. This similar to the 50-65 TgC we estimate for JJA 2018, which in turn agrees closely with our earlier estimate (49.8 TgC over the blue (including the blue/yellow hatched) area in Fig 2) for that event[30]. The quoted range includes one mechanistic model calculation (SiB4) from our CTE-HR near real-time flux product for Europe[31], as well as preliminary results from atmospheric inverse modeling with a limited set of observation sites (see Supplement D). We note that such an atmospheric inverse modeling estimate is a time-consuming task, requiring several inputs that are not directly available, and therefore inverse fluxes are typically not available until a year after such an event, while CTE-HR results are available within one week after real-time. The close correspondence of the inverse results and the bioshere model calculations, reconfirms the capacity of the underlying SiB4 biosphere model to convincingly capture the summer drought impact on European NEE, as we also reported in Smith et al. (2020)[30].

Regionally, we find the central (blue-yellow hatched) area in Fig. 2 that was hit twice by summer droughts to have responded

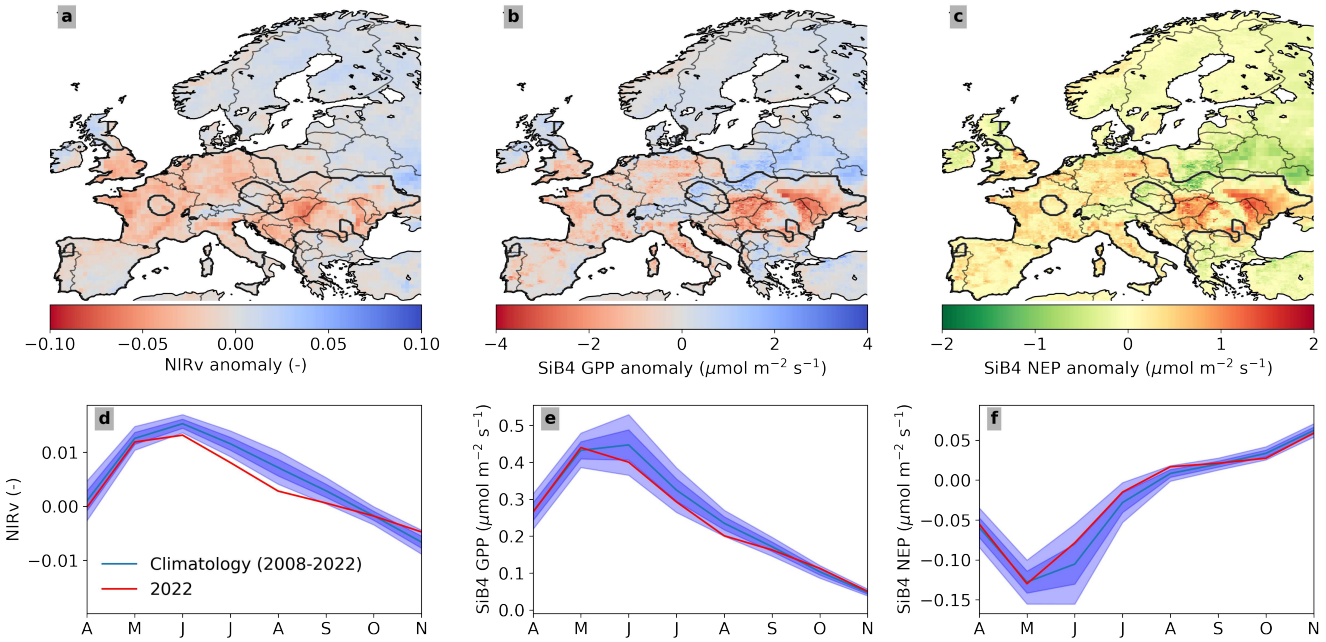

Figure 4. Spatial distribution of mean anomalies during the months June, July and August 2022 for detrended near-infrared reflectance of vegetation (NIRv, a) calculated from MODIS surface reflectance, gross primary production (GPP, b) simulated by the SiB4 biosphere model, and Net Ecosystem Production (NEP, c) simulated by the SiB4 biosphere model. The climatology is based on 2008–2022. Monthly mean values of the 2022 anomalies over the entire 2022 drought region (indicated by the black contours) from April to November are shown underneath each corresponding map (d-f) in red. The climatology and its one and two-sigma bandwidth are indicated in blue.

less strongly in JJA 2022 (an anomaly of 7.8 TgC in 2022 and 19.7 TgC in 2018), but also experienced at a slightly less extreme drought (SPEI of -1.66 in 2022 versus -1.98 in 2018). The role of delayed and compound effects of multiple warm and dry preceding summers on these needs more detailed analysis in a future study. In the South (yellow) region, we find, per unit area, a smaller response in 2022 compared to the North (blue) region in 2018 (2.0 and 3.0 gC m^{-2} $month^{-1}$, respectively), even though the South locally experienced more extreme conditions (mean 3-month SPEI of -1.88 and -1.68, and average VPD of 13.6 and 5.1 hPa, respectively). We argue that this signifies a higher drought tolerance of the southern European vegetation, which is likely to be better adapted to high mean temperatures and low moisture availability than the northern forests hit in 2018[32,33].

Finally, the East (red) region, which was impacted only in 2022, contributed most to the net ecosystem productivity (NEP) anomaly in the drought-influenced area (76%). This is a result that is based on the SiB4 model calculations, made necessary by a lack of sufficient atmospheric observation sites in the East. This gap in our monitoring capacity, also quantified in[34], limits our understanding of drought impacts on net carbon uptake across pan-European forests, and will hamper the desired independent verification of forest carbon sequestration across the EU.

Forest productivity

Reduced net carbon uptake in summer is a combination of reduced Gross Primary Productivity (GPP), partly balanced by reduced Terrestrial Ecosystem Respiration (TER)[35]. Reduced GPP results from a well-known mechanism to increase leaf-level water-use efficiency and reduce evaporative loss at the expense of carbon assimilation, detectable at leaf, ecosystem, and continental scale[36–38]. This in turn affects the canopy structure and leads to sub-optimal interception of sunlight and widespread reductions in the reflection of near-infrared reflection by vegetation (NIRv[39]) which scales highly linearly with GPP[39]. For an extensive analysis of NIRv, see Supplementary Section F. This NIRv reduction is shown in Fig. 4, and independently confirms large impacts on carbon uptake by vegetation across the southern, eastern and central region. The year 2022 ranks 1st or 2nd (behind 2018, depending on the gridcell) in magnitude over the 2000-2022 NIRv record (see Supplementary Fig. S9. Moreover, it highlights the eastern European region as a key impacted area with an unprecedentedly low summer NIRv on record. This partly results from the 2022 drought already starting in spring of 2022 in eastern Europe, propagating slowly towards the center of the East area in Fig 2, and further intensifying in June (see Supplementary Fig. S8).

Following the approach we introduced in Smith et al.[30], we convert the anomaly in NIRv to GPP using its biome-specific

Table 1. Meteorological and flux anomalies at forest EC sites during summer (JJA) and autumn (SON) of 2022, relative to 2019-2021 for gross primary production (GPP), net ecosystem exchange (NEE), total ecosystem respiration (TER), Standardized precipitation and evaporation index (SPEI) and vapour pressure deficit (VPD).

	GPP (μmol m^{-2} s^{-1})		NEE (μmol m^{-2} s^{-1})		TER (μmol m^{-2} s^{-1})		SPEI (-)		VPD (hPa)	
	JJA	SON	JJA	SON	JJA	SON	JJA	SON	JJA	SON
Station name										
DK-Sor	-2.12	0.60	0.89	-0.60	-1.27	-0.03	-0.21	-1.37	1.22	0.48
IT-SR2	-3.62	-2.92	2.20	0.55	-1.54	-2.32	-0.67	-0.39	1.97	1.09
FI-Hyy	2.11	1.34	-1.56	-1.11	0.55	0.23	-0.93	-0.98	1.14	0.16
BE-Bra	1.42	-	-1.52	-	-0.10	-	-0.78	-	0.95	-
FR-FBn	-1.93	2.48	1.81	-1.83	-0.12	0.65	0.40	0.21	1.96	0.11
FR-Pue	-2.33	1.49	1.56	-0.64	-0.77	0.85	-0.94	-0.00	6.38	-1.39
FR-Fon	2.30	1.70	-2.12	-1.08	0.18	0.61	-1.51	-0.16	4.11	-0.41
FR-Hes	-3.19	0.33	1.67	0.01	-1.52	0.32	-1.57	0.11	3.44	-1.05
SE-Htm	0.25	1.51	-0.38	-0.92	-0.10	0.62	-1.64	-1.68	2.01	0.60
DE-Tha	-1.64	0.71	1.44	-0.67	-0.20	0.03	-0.79	1.03	3.89	1.74
CH-Dav	-2.01	-0.44	-0.04	-0.05	-1.96	-0.38	-1.74	-1.70	1.86	0.72
BE-Vie	-0.30	0.36	0.20	0.55	-0.11	0.92	-1.70	-0.48	3.30	0.04
FR-Bil	-6.32	-1.60	4.32	1.11	-1.97	-0.50	-0.25	0.76	7.57	1.44
DE-HoH	-2.31	-0.31	1.35	-0.52	-0.67	-0.37	-0.44	-0.35	2.95	0.76

linear relation to GPP derived from eddy-covariance observations (see Suppl. Info F). This results in averaged JJA reductions of -44.1 $\pm$ 16.4 / -50.7 $\pm$ 18.2 / -47.3 $\pm$ 17.8 TgC/month over the Centre, South and Eastern region, respectively over the three summer months. Forests contributed 31.5 $\pm$ 11.1 TgC to this GPP anomaly (-8.2 $\pm$ 3.0 / -10.0 $\pm$ 3.4 / -13.3 $\pm$ 4.5), corroborating the better resilience to drought than European grasslands and croplands found previously by Teuling et al (2010)[40]. Independently, SiB4 calculates GPP-anomaly patterns highly similar to the observed NIRv (spatial correlation of R=0.78, N=41, p=10^{-9}, see Supplementary material G), integrating to 12 / 18 / 25 TgC/month for the same areas. Furthermore, the agreement with the EC-measurements at point scale (see Supplementary Fig. S12) lends further credibility to our analyses of the underlying drought response of GPP using SiB4, which we provide next.

Vapour pressure deficit vs Soil moisture

Our SiB4 results indicate that large atmospheric vapor pressure deficits are the dominant cause of reduced GPP in the southern and central regions in July-August 2022, while soil moisture deficits underlie the strongest impacts in eastern Europe. This is illustrated in Fig. 5, which shows the relative importance of three calculated vegetation stress factors (excess heat, high VPD, deficit in root-zone soil moisture) for July and August of 2022, along with those of 2018. Soil moisture deficits, responsible for the most intense impacts on GPP in 2018, have played a smaller role in the central region in 2022 and were not the dominant driver of GPP reductions in southern France and Italy, where impacts were nevertheless high in 2022.

The important role of VPD in the southern and central regions is independently confirmed by local EC-observations, but soil moisture observations of sufficient quality and continuity were not available. At the EC towers that experienced above-average VPD, GPP is reduced by 37% (also see Table 1 and Supplementary Fig. S12). Furthermore, Fig. 5 indicates the extreme GPP anomaly for 2022 for the selected sites is mainly in the South region. Reduced GPP is often paired with a reduction in ecosystem respiration[19,30,41]. These countering effects reduce the impact of the drought on the net ecosystem exchange. Nevertheless, some sites that were most severely struck by the drought (FR-Bil and FR-Pue) became a net source of CO_2 during JJA of 2022. This switch from sink to source of carbon sink during summer has not been observed before, and proves that extreme conditions can cause carbon loss to the atmosphere even during the growing season. Moreover, if heat and atmospheric moisture demand are the main drivers, the extremes that drove the 2022 reversal will become part of normal climatological conditions as climate warming persists[17,42].

EC-observations that could confirm the dominance of soil moisture limitations calculated by SiB4 (Fig. 5) are lacking for the eastern region, but strong soil moisture depletion is simulated by ERA-Land[21] and observed through SMAP L-band satellite observations[43] of top-level soil moisture (Fig S2, SMAP not shown). Depleted soil moisture is also very plausible given the early start of rainfall deficits in the eastern region. We see this as another example of the importance of spring-summer legacy effects in carbon uptake[30,44,45], but confirmation with local observations and more intense monitoring is needed to truly understand the driving mechanism.

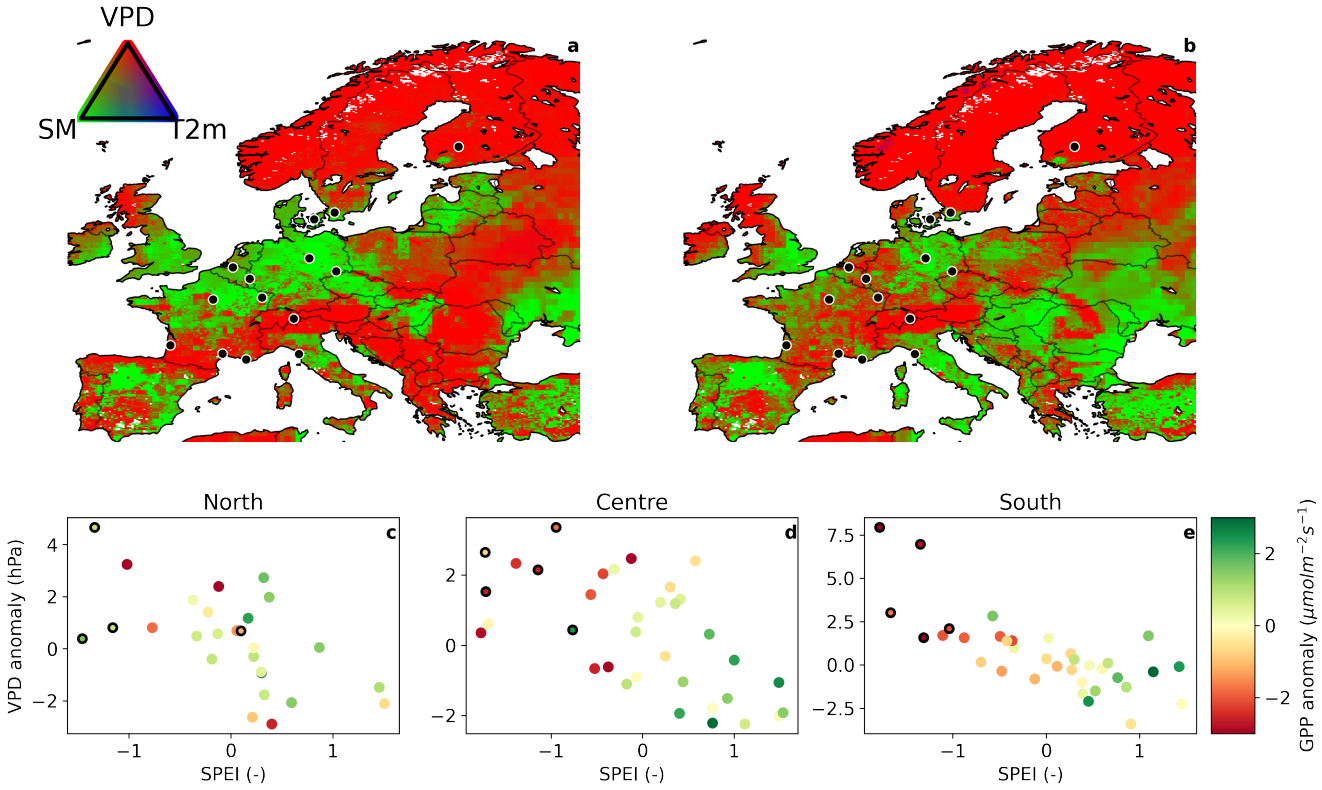

Figure 5. Dominant stress factors (VPD: atmospheric drought; SM: Soil moisture; T2m: temperature) for July and August 2018 (left) and 2022 (right) in the SiB4 model (see Supplementary Section G.3). The EC sites used are indicated by black dots. Bottom row: 3-month SPEI, averaged over July and August and VPD anomalies at available EC sites in different regions (Supplementary Table S3) for the years 2016-2022, with 2022 marked with a black contour. Colours indicate measured GPP anomalies with respect to 2016-2022.

Warm autumn compensation

Besides the warm summer, 2022 also experienced the warmest autumn on record in Europe[3]. This warm autumn was accompanied by replenished soil water over large parts of the drought-affected area[3](see also Supplementary Fig. S1). These conditions led to delayed leaf senescence, as seen by NIRv (Figures S8 and S10) and at EC sites (Table 1). The higher than normal NIRv is estimated to account for 66 $\pm$ 12 TgC/month higher GPP in October and November which is roughly 30% above normal. At the same time, mean atmospheric CO_2 mole fractions were 0.89 ppm lower than normal at the used stations (Fig. 3), suggesting enhanced CO_2 uptake during the warm autumn and possible result in a partial compensation for the reduced summer net carbon uptake. However, a large fraction of these CO_2 anomalies are driven by advection of southerly air that was relatively low in CO_2 as also indicated by lower CO and CH_4 at these stations (Fig. S4) and an atmospheric transport quantification of this influence (Supplementary Table S2).

We calculate that the enhanced uptake in October and November compensates up to 32% of the reduced uptake during the summer in the Centre and South region, much smaller than the 2018 warm spring compensation of $\pm$75% found for 2018[30,44,45]. The lesser effect of a warm autumn compared to spring has also been found in deciduous forests[46], where better growing conditions in spring promote GPP more than TER, potentially due to the higher soil moisture and incoming radiation in spring[46]. Moreover, the mechanisms of enhanced autumn and spring uptake differ. Enhanced autumn uptake is controlled by late leaf senescence and continued photosynthesis in regions with sufficient light and heat[47,48], while enhanced spring carbon uptake is caused by early snow-melt and advanced accumulation of the temperature threshold for leaf-out, and plentiful sunlight[49,50]. In both mechanisms, accumulated impacts (i.e. higher than normal temperatures or incoming radiation due to lower cloud cover) affect phenology of vegetation. This is a difficult process to simulate mechanistically[47,50] as evidenced by the poorer performance of SiB4, as well as other vegetation models (see Suppl S15) in autumn 2022. Note that we could not constrain this effect for the East region due to lack of measurements.

Fires

Although in the Les Landes region in the south-west of France the drought spurred exceptionally large wildfires, the total loss of carbon through fires in Europe in 2022 is thought to be small (14.6-16.0 TgC, see Supplementary information I). VIIRS active fire counts[51] for the year 2022 show a positive anomaly relative to the previous 20 years, ranking 4th with total detections until August (Fig S18). They similarly show a high anomaly in France, equivalent in magnitude to 2003 that had a similar water deficit and peak temperature. Importantly, in 2003 the fire anomaly occurred in Mediterranean areas whereas it took place in temperate areas during 2022 with the Les Landes forests (Fig S16). This resulted in more biomass burned per unit area in 2022 compared to 2003.

An assessment of these fires in France, based on Sentinel-2 observations of burned area at a 10m resolution and a 10 m map of impacted biomass density derived from Global Ecosystem Dynamics Investigation (GEDI) height and French National forest inventory (NFI) plot data was produced by Vallet et al.[52]. Vallet et al.[52] did not calculate emissions, but biomass lost from fires. Emissions of carbon gases and aerosols to the atmosphere should represent at most 50% of the biomass lost[52], given typical combustion completeness factors. Our best estimate of biomass loss derived from this study is of 0.5 Tg C y^{-1}. Specific to the fire season 2022 in France was that frequently burned Mediterranean forests and shrublands did not show an anomaly, but extreme fires occurred in regions where they have not been observed before (Atlantic pine forests in the South West, Brittany, Loire valley and Jura), affecting temperate forests with higher biomass, and thus leading to larger biomass loss rates. Although strongly affecting emissions from France, fires seem to have played a smaller role across the rest of Europe.

Despite high temperatures and extended drought, at European scale, the year 2022 only ranks 5th on record for GFAS (2003-2022) carbon emissions[28]. It was characterized by below-normal emissions from March to June, followed by a fast rise in July, with a peak at 4.5 Tg C $month^{-1}$, which shows the highest July fire rate observed (Fig S17). At country scale, the largest fire flux was in Spain with emissions of 1.8 Tg C $month^{-1}$ in July, accounting for 40% of the European emissions in that month. The second largest fire emissions emissions were in Portugal, peaking in August at (0.8 Tg C $month^{-1}$), about equal to France in July (0.6 Tg C $month^{-1}$). The integrated additional loss of carbon to the atmosphere from fires in 2022 is 5.2 TgC yr^{-1} over the drought regions identified in this study. Compared to 2003, the fire emissions over the entirety of Europe are very similar (15.2 and 14.6 TgC yr^{-1} in 2003 and 2022, respectively), with 2003 having its peak carbon loss from fires in August (see also Supplementary Fig. S17.

Discussion

We find a 2022 summer reduction of NEP of 57-62 TgC over the drought-affected area, which is similar to the reduced NEP in the summer of 2018 (50-65 TgC). But contrary to the drought of 2018, we do not find a large offset of this reduced uptake outside of the growing season as found previously[30,44,45]. This thus suggests a larger impact on the European carbon budget overall, with GPP anomalies (derived from NIRv and EC observations) over the drought-affected area over the growing season almost 50% higher in 2022 than in 2018 (see Supplementary Section F). Also, fires played a substantially larger part in carbon

loss from forests than in 2018. Together, these two droughts show a substantial response of the European forest sink of CO_2 to drought, with the absence of favorable spring conditions and intensity of atmospheric heat and moisture deficits in summer as exacerbating factors.

Recent studies of tree-level responses to the 2018 drought have also shown this vulnerability of forest ecosystems to droughts[53]. Especially beech forests were found to be vulnerable[54,55]. Many of these beech forests reside in the East region[56], which is a poorly monitored part of Europe[34]. With beech forests projected to have a growth reduction up to 90% by 2090 in areas that are projected to experience more severe droughts[55], it is imperative to better observe these forests.

Forest vulnerability to drought was also found in Haberstroh et al.,[57], who found 47% of their 368 Scots pine trees to have died in 2020, due to legacy after the 2018 drought. Also Senf et al.[58] found reduced resilience due to drought, indicating persistent effects of drought. In this first assessment of the drought of 2022, we could not account for such legacy effects, that will likely play out in the next few years. Therefore, these legacy effects could potentially aggravate the effects of the 2022 drought. These legacy effects should therefore be further explored in future studies, as should potential compound effects[45,59], such as the warm winter of 2022-2023.

Our study, which we have carried out from the atmospheric perspective, also shows a critical role of TER and soil moisture for the drought response. We find a strong reduction of GPP, but lower NEP reductions, indicating a reduction in TER as well. However, contrary to GPP, which can be estimated from satellite products, TER cannot currently be quantified on a large scale. Nevertheless, EC observations show reduced TER with reduced GPP due to the drought in the South region in 2022. In contrast, we find a strong GPP response in the centre region, but no corresponding TER response (Supplementary Fig. S7). Although we currently cannot verify this, we hypothesise that the lack of TER response is due to the strong VPD limitation on GPP, but no strong soil moisture limitation on TER. This shows the importance of TER for total ecosystem response to drought, and the difference between soil moisture and VPD-driven droughts. However, these findings are not backed up by the biosphere models, possibly because TER parameterisations in biosphere models (mainly temperature-based) do not fully capture the actual TER response[60,61].

Due to a lack of direct observations, our current results in the eastern region are based mostly on the biosphere model SiB4[61], downscaled to a higher resolution[31]. SiB4 was found to simulate the NEP response to droughts well in central and northern Europe[30,31], and also in this work its calculations agree well with observed atmospheric and EC-based anomalies where available (see Supplementary Figures S5 and S12). Nevertheless, the lack of CO_2 observing capacity, both in atmospheric CO_2 and ecosystem exchange over eastern European forests, as also indicated by[34,62], remains worrisome. Especially eastern European forests could become an important part of the EU's goal to net-zero greenhouse gas emissions[63] but remain understudied until more extensive monitoring is realized. Most importantly, the impact of more frequent events like 2018 and 2022 need to be factored into potential carbon sequestration calculations by these, and other European forests[64].

Despite the mentioned limitations in the European carbon cycle monitoring, we also show in this study that with the build-up of ICOS, the infrastructure is present to analyse and quantify a major event in the European carbon cycle in near-real time. All atmospheric measurements, eddy-covariance measurements, satellite observations and model results we presented were available within a few days to maximally 3 months behind real-time. This is a stark improvement over the analysis of the 2018 drought that was concluded nearly 24 months after the event[20]. Especially, this offers good prospects for continuous integrated monitoring of the European carbon balance, aimed for by the EU's Copernicus program[65].

References

1. Copernicus. Copernicus: Summer 2022 Europe's hottest on record. *Copernicus* (2022).

2. Toreti, A. *et al.* Drought in Europe August 2022. Tech. Rep. KJ-NA-31-192-EN-N (online), Luxembourg (Luxembourg) (2022). DOI: 10.2760/264241(online).

3. S, B. *et al.* JRC MARS Bulletin - Crop monitoring in Europe - November 2022 Vol. 30 No 11. Scientific analysis or review KJ-AW-22-011-EN-N (online), Luxembourg (Luxembourg) (2022). DOI: 10.2760/825311(online).

4. Kornhuber, K. *et al.* Extreme weather events in early summer 2018 connected by a recurrent hemispheric wave-7 pattern. *Environ. Res. Lett.* **14**, 054002, DOI: 10.1088/1748-9326/ab13bf (2019-04).

5. Barriopedro, D., Sousa, P. M., Trigo, R. M., García-Herrera, R. & Ramos, A. M. The Exceptional Iberian Heatwave of Summer 2018. *Bull. Am. Meteorol. Soc.* **101**, S29–S34, DOI: 10.1175/BAMS-D-19-0159.1 (2020).

6. Liu, X., He, B., Guo, L., Huang, L. & Chen, D. Similarities and Differences in the Mechanisms Causing the European Summer Heatwaves in 2003, 2010, and 2018. *Earth's Futur.* **8**, e2019EF001386, DOI: 10.1029/2019EF001386 (2020).

7. Vicente-Serrano, S. M. & López-Moreno, J. I. Nonstationary influence of the North Atlantic Oscillation on European precipitation. *J. Geophys. Res.* **113**, D20120, DOI: 10.1029/2008JD010382 (2008).

8. Ionita, M., Nagavciuc, V., Scholz, P. & Dima, M. Long-term drought intensification over Europe driven by the weakening trend of the Atlantic Meridional Overturning Circulation. *J. Hydrol. Reg. Stud.* **42**, 101176, DOI: 10.1016/j.ejrh.2022.101176 (2022).

9. Fischer, E. M., Seneviratne, S. I., Lüthi, D. & Schär, C. Contribution of land-atmosphere coupling to recent European summer heat waves. *Geophys. Res. Lett.* **34**, L02202, DOI: 10.1029/2006gl029068 (2007).

10. Hanel, M. *et al.* Revisiting the recent European droughts from a long-term perspective. *Sci. Reports* **8**, 9499, DOI: 10.1038/s41598-018-27464-4 (2018).

11. Drouard, M., Kornhuber, K. & Woollings, T. Disentangling Dynamic Contributions to Summer 2018 Anomalous Weather Over Europe. *Geophys. Res. Lett.* **46**, 12537–12546, DOI: 10.1029/2019GL084601 (2019).

12. Buras, A., Rammig, A. & Zang, C. S. Quantifying impacts of the 2018 drought on European ecosystems in comparison to 2003. *Biogeosciences* **17**, 1655–1672, DOI: 10.5194/bg-17-1655-2020 (2020).

13. Samaniego, L. *et al.* Anthropogenic warming exacerbates European soil moisture droughts. *Nat. Publ. Group* **8**, 421 – 426, DOI: 10.1038/s41558-018-0138-5 (2018).

14. Rasmijn, L. M. *et al.* Future equivalent of 2010 Russian heatwave intensified by weakening soil moisture constraints (2018).

15. Spinoni, J., Vogt, J. V., Naumann, G., Barbosa, P. & Dosio, A. Will drought events become more frequent and severe in Europe? *Int. J. Climatol.* **38**, 1718–1736, DOI: 10.1002/joc.5291 (2018).

16. Schumacher, D. L. *et al.* Amplification of mega-heatwaves through heat torrents fuelled by upwind drought. *Nat. Geosci.* **12**, 712 – 717, DOI: 10.1038/s41561-019-0431-6 (2019).

17. Hari, V., Rakovec, O., Markonis, Y., Hanel, M. & Kumar, R. Increased future occurrences of the exceptional 2018–2019 Central European drought under global warming. *Sci. Reports* **10**, 12207, DOI: 10.1038/s41598-020-68872-9 (2020).

18. Robine, J. M. *et al.* Death toll exceeded 70,000 in Europe during the summer of 2003. *Comptes Rendus Biol.* **331**, 171–178, DOI: 10.1016/J.CRVI.2007.12.001 (2008).

19. Ciais, P. P. *et al.* Europe-wide reduction in primary productivity caused by the heat and drought in 2003. *Nature* **437**, 529 – 533, DOI: 10.1038/nature03972 (2005).

20. Peters, W., Bastos, A., Ciais, P. & Vermeulen, A. A historical, geographical and ecological perspective on the 2018 European summer drought. *Philos. Transactions Royal Soc. B* **375**, 20190505, DOI: 10.1098/rstb.2019.0505 (2020).

21. Muñoz-Sabater, J. *et al.* ERA5-Land: a state-of-the-art global reanalysis dataset for land applications. *Earth Syst. Sci. Data* **13**, 4349–4383, DOI: 10.5194/essd-13-4349-2021 (2021).

22. Hersbach, H. *et al.* The ERA5 global reanalysis. *Q. J. Royal Meteorol. Soc.* **146**, 1999–2049, DOI: 10.1002/qj.3803 (2020).

23. Vautard, R. *et al.* Summertime European heat and drought waves induced by wintertime Mediterranean rainfall deficit. *Geophys. Res. Lett.* **34**, DOI: 10.1029/2006gl028001 (2007).

24. Quesada, B., Vautard, R., Yiou, P., Hirschi, M. & Seneviratne, S. I. Asymmetric European summer heat predictability from wet and dry southern winters and springs. *Nat. Publ. Group* **2**, 736 – 741, DOI: 10.1038/nclimate1536 (2012).

25. Miralles, D. G., Teuling, A. J., van Heerwaarden, C. C. & Vilà-Guerau de Arellano, J. Mega-heatwave temperatures due to combined soil desiccation and atmospheric heat accumulation. *Nat. Geosci.* **7**, 345–349, DOI: 10.1038/ngeo2141 (2014).

26. Dirmeyer, P. A., Balsamo, G., Blyth, E. M., Morrison, R. & Cooper, H. M. Land-Atmosphere Interactions Exacerbated the Drought and Heatwave Over Northern Europe During Summer 2018. *AGU Adv.* **2**, DOI: 10.1029/2020av000283 (2021).

27. Zhou, S. *et al.* Land–atmosphere feedbacks exacerbate concurrent soil drought and atmospheric aridity. *Proc. Natl. Acad. Sci.* **116**, 18848–18853, DOI: 10.1073/pnas.1904955116 (2019).

28. Di Giuseppe, F., Rémy, S., Pappenberger, F. & Wetterhall, F. Combining fire radiative power observations with the fire weather index improves the estimation of fire emissions. *Atmospheric Chem. Phys. Discuss.* 1–16, DOI: 10.5194/acp-2017-790 (2017).

29. Heiskanen, J. *et al.* The Integrated Carbon Observation System in Europe. *Bull. Am. Meteorol. Soc.* **103**, E855–E872, DOI: 10.1175/BAMS-D-19-0364.1 (2022).

30. Smith, N. E. *et al.* Spring enhancement and summer reduction in carbon uptake during the 2018 drought in northwestern Europe. *Philos. Transactions Royal Soc. B* **375**, 20190509, DOI: 10.1098/rstb.2019.0509 (2020).

31. van der Woude, A. M. *et al.* Near real-time CO_2 fluxes from CarbonTracker Europe for high resolution atmospheric modeling. *Earth Syst. Sci. Data Discuss.* **2022**, 1–38, DOI: 10.5194/ESSD-15-579-2023 (2022).

32. Gazol, A. *et al.* Forest resilience to drought varies across biomes. *Glob. Chang. Biol.* **24**, 2143–2158, DOI: 10.1111/gcb.14082 (2018).

33. Gazol, A., Camarero, J. J., Anderegg, W. R. L. & Vicente-Serrano, S. M. Impacts of droughts on the growth resilience of Northern Hemisphere forests. *Glob. Ecol. Biogeogr.* **26**, 166–176, DOI: 10.1111/geb.12526 (2017).

34. Storm, I., Karstens, U., D'Onofrio, C., Vermeulen, A. & Peters, W. A view of the European carbon flux landscape through the lens of the ICOS atmospheric observation network. *Atmospheric Chem. Phys. Discuss.* **2022**, 1–25, DOI: 10.5194/acp-2022-756 (2022).

35. Pereira, J. S. *et al.* Net ecosystem carbon exchange in three contrasting Mediterranean ecosystems – the effect of drought. *Biogeosciences* **4**, 791–802, DOI: 10.5194/bg-4-791-2007 (2007).

36. Beer, C. *et al.* Temporal and among-site variability of inherent water use efficiency at the ecosystem level. *Glob. Biogeochem. Cycles* **23**, n/a–n/a, DOI: 10.1029/2008GB003233 (2009).

37. Medrano, H., Flexas, J. & Galmés, J. Variability in water use efficiency at the leaf level among Mediterranean plants with different growth forms. *Plant Soil* **317**, 17–29, DOI: 10.1007/s11104-008-9785-z (2009).

38. Peters, W. *et al.* Increased water-use efficiency and reduced CO2 uptake by plants during droughts at a continental scale. *Nat. Geosci.* **11**, 744–748, DOI: 10.1038/s41561-018-0212-7 (2018).

39. Badgley, G., Field, C. B. & Berry, J. A. Canopy near-infrared reflectance and terrestrial photosynthesis. *Sci. Adv.* **3**, e1602244, DOI: 10.1126/sciadv.1602244 (2017).

40. Teuling, A. J. *et al.* Contrasting response of European forest and grassland energy exchange to heatwaves. *Nat. Geosci.* **3**, 722 – 727, DOI: 10.1038/ngeo950 (2010).

41. Von Buttlar, J. *et al.* Impacts of droughts and extreme-temperature events on gross primary production and ecosystem respiration: A systematic assessment across ecosystems and climate zones. *Biogeosciences* **15**, 1293–1318, DOI: 10.5194/BG-15-1293-2018 (2018).

42. Fu, Z. *et al.* Uncovering the critical soil moisture thresholds of plant water stress for European ecosystems. *Glob. Chang. Biol.* **28**, 2111–2123, DOI: 10.1111/gcb.16050 (2022).

43. Entekhabi, D., Njoku, E. & O'Neill, P. The Soil Moisture Active and Passive Mission (SMAP): Science and applications. In *2009 IEEE Radar Conference*, vol. 674, 1–3, DOI: 10.1109/RADAR.2009.4977030 (IEEE, 2009).

44. Wolf, S. *et al.* Warm spring reduced carbon cycle impact of the 2012 US summer drought. *Proc. Natl. Acad. Sci.* **113**, 5880–5885, DOI: 10.1073/pnas.1519620113 (2016).

45. Bastos, A. *et al.* Direct and seasonal legacy effects of the 2018 heat wave and drought on European ecosystem productivity. *Sci. Adv.* **6**, eaba2724, DOI: 10.1126/sciadv.aba2724 (2020).

46. Teets, A. *et al.* Early spring onset increases carbon uptake more than late fall senescence: modeling future phenological change in a US northern deciduous forest. *Oecologia* **201**, 241–257, DOI: 10.1007/s00442-022-05296-4 (2023).

47. Lang, W., Chen, X., Qian, S., Liu, G. & Piao, S. A new process-based model for predicting autumn phenology: How is leaf senescence controlled by photoperiod and temperature coupling? *Agric. For. Meteorol.* **268**, 124–135, DOI: 10.1016/j.agrformet.2019.01.006 (2019).

48. Polgar, C. A. & Primack, R. B. Leaf-out phenology of temperate woody plants: from trees to ecosystems. *New Phytol.* **191**, 926–941, DOI: 10.1111/j.1469-8137.2011.03803.x (2011).

49. Fu, Y. H. *et al.* Larger temperature response of autumn leaf senescence than spring leaf-out phenology. *Glob. Chang. Biol.* **24**, 2159–2168, DOI: 10.1111/gcb.14021 (2018).

50. Fu, Y. *et al.* Progress in plant phenology modeling under global climate change. *Sci. China Earth Sci.* **63**, 1237–1247, DOI: 10.1007/s11430-019-9622-2 (2020).

51. Schroeder, W. & Giglio, L. NASA VIIRS Land Science Investigator Processing System (SIPS) Visible Infrared Imaging Radiometer Suite (VIIRS) 375 m & 750 m Active Fire Products: Product User's Guide Version 1.4 (2018).

52. Vallet, L. *et al.* High resolution data reveal a surge of biomass loss from temperate and Atlantic pine forests, seizing the 2022 fire season distinctiveness in France. *EGUsphere* **2023**, 1–39, DOI: 10.5194/egusphere-2023-529 (2023).

53. Schuldt, B. & Ruehr, N. K. Responses of European forests to global change-type droughts. *Plant Biol.* **24**, 1093–1097, DOI: 10.1111/plb.13484 (2022).

54. Frei, E. R. *et al.* European beech dieback after premature leaf senescence during the 2018 drought in northern Switzerland. *Plant Biol.* **24**, 1132–1145, DOI: 10.1111/plb.13467 (2022).

55. Martinez del Castillo, E. *et al.* Climate-change-driven growth decline of European beech forests. *Commun. Biol.* **5**, 163, DOI: 10.1038/s42003-022-03107-3 (2022).

56. European Environment Agency. map 3-1 european-forests-new.eps — European Environment Agency (2009).

57. Haberstroh, S. *et al.* Central European 2018 hot drought shifts scots pine forest to its tipping point. *Plant Biol.* **24**, 1186–1197, DOI: 10.1111/plb.13455 (2022).

58. Senf, C. & Seidl, R. Persistent impacts of the 2018 drought on forest disturbance regimes in Europe. *Biogeosciences* **18**, 5223–5230, DOI: 10.5194/bg-18-5223-2021 (2021).

59. Gazol, A. & Camarero, J. J. Compound climate events increase tree drought mortality across European forests. *Sci. The Total. Environ.* **816**, 151604, DOI: 10.1016/j.scitotenv.2021.151604 (2022).

60. Clark, D. B. *et al.* The Joint UK Land Environment Simulator (JULES), model description – Part 2: Carbon fluxes and vegetation dynamics. *Geosci. Model. Dev.* **4**, 701–722, DOI: 10.5194/gmd-4-701-2011 (2011).

61. Haynes, K., Baker, I. & Denning, A. S. The Simple Biosphere Model, Version 4.2: SiB4 Technical description. *Colo. State Univ.* (2020).

62. Spinoni, J. *et al.* An overview of drought events in the Carpathian Region in 1961–2010. *Adv. Sci. Res.* **10**, 21–32, DOI: 10.5194/asr-10-21-2013 (2013).

63. Pilli, R., Alkama, R., Cescatti, A., Kurz, W. A. & Grassi, G. The European forest carbon budget under future climate conditions and current management practices. *Biogeosciences* **19**, 3263–3284, DOI: 10.5194/bg-19-3263-2022 (2022).

64. Anderegg, W. R. L. *et al.* A climate risk analysis of Earth's forests in the 21st century. *Science* **377**, 1099–1103, DOI: 10.1126/science.abp9723 (2022).

65. Balsamo, G. *et al.* The CO2 Human Emissions (CHE) Project: First Steps Towards a European Operational Capacity to Monitor Anthropogenic CO2 Emissions. *Front. Remote. Sens.* **2**, 707247, DOI: 10.3389/frsen.2021.707247 (2021).

66. Avitabile, V. *et al. Comparative analysis and fusion for improved global biomass mapping*, 251—-255 (2014).

67. ICOS RI *et al.* European Obspack compilation of atmospheric carbon dioxide data from ICOS and non-ICOS European stations for the period 1972-2022; obspack_co2_466_GLOBALVIEWplus_v8.0_2023-03-30, DOI: 10.18160/CEC4-CAGK (2023).

68. Munassar, S. *et al.* Net ecosystem exchange (NEE) estimates 2006–2019 over Europe from a pre-operational ensemble-inversion system. *Atmospheric Chem. Phys.* **22**, 7875–7892, DOI: 10.5194/acp-22-7875-2022 (2022).

69. Lin, J. C. *et al.* A near-field tool for simulating the upstream influence of atmospheric observations: The Stochastic Time-Inverted Lagrangian Transport (STILT) model. *J. Geophys. Res. Atmospheres* **108**, 4493, DOI: 10.1029/2002jd003161 (2003).

70. Friedlingstein, P. *et al.* Global Carbon Budget 2021. *Earth Syst. Sci. Data* **14**, 1917–2005, DOI: 10.5194/essd-14-1917-2022 (2022).

71. Peters, W. *et al.* An ensemble data assimilation system to estimate CO 2 surface fluxes from atmospheric trace gas observations. *J. Geophys. Res.* **110**, D24304, DOI: 10.1029/2005JD006157 (2005).

72. Munassar, S. *et al.* Why do inverse models disagree? A case study with two European CO 2 inversions. *Atmospheric Chem. Phys.* **23**, 2813–2828, DOI: 10.5194/acp-23-2813-2023 (2023).

73. Krol, M. *et al.* The two-way nested global chemistry-transport zoom model TM5: algorithm and applications. *Atmospheric Chem. Phys.* **5**, 417–432, DOI: 10.5194/acp-5-417-2005 (2005).

74. Warm Winter 2020 Team & ICOS Ecosystem Thematic Centre. Warm winter 2020 ecosystem eddy covariance flux product for 73 stations in fluxnet-archive format—release 2022-1, DOI: 10.18160/2G60-ZHAK (2020).

75. Sabbatini, S. *et al.* Eddy covariance raw data processing for CO2 and energy fluxes calculation at ICOS ecosystem stations. *Int. Agrophysics* **32**, 495–515, DOI: 10.1515/intag-2017-0043 (2018).

76. Pastorello, G. *et al.* The FLUXNET2015 dataset and the ONEFlux processing pipeline for eddy covariance data. *Sci. Data* **7**, 225, DOI: 10.1038/s41597-020-0534-3 (2020).

77. Turner, A. J. *et al.* A double peak in the seasonality of California's photosynthesis as observed from space. *Biogeosciences* **17**, 405–422, DOI: 10.5194/bg-17-405-2020 (2020).

78. Mengistu, A. G. *et al.* Sun-induced fluorescence and near-infrared reflectance of vegetation track the seasonal dynamics of gross primary production over Africa. *Biogeosciences* **18**, 2843–2857, DOI: 10.5194/bg-18-2843-2021 (2021).

79. Buitink, J. *et al.* Anatomy of the 2018 agricultural drought in the Netherlands using in situ soil moisture and satellite vegetation indices. *Hydrol. Earth Syst. Sci.* **24**, 6021–6031, DOI: 10.5194/hess-24-6021-2020 (2020).

80. Schaaf, C. & Wang, Z. CD43C4 MODIS/Terra+Aqua BRDF/Albedo Nadir BRDF-Adjusted Ref Daily L3 Global 0.05Deg CMG V006 [data set], DOI: https://doi.org/10.5067/MODIS/MCD43C4.006 (2015).

81. Bossard, M., Feranec, J. & Otahel, J. CORINE land cover technical guide – Addendum 2000 Part I State-of-play production methods of the CORINE land cover database (2000).

82. Zaehle, S. & Friend, A. D. Carbon and nitrogen cycle dynamics in the O-CN land surface model: 1. Model description, site-scale evaluation, and sensitivity to parameter estimates. *Glob. Biogeochem. Cycles* **24**, n/a–n/a, DOI: 10.1029/2009GB003521 (2010).

83. Di Giuseppe, F., Rémy, S., Pappenberger, F. & Wetterhall, F. Using the Fire Weather Index (FWI) to improve the estimation of fire emissions from fire radiative power (FRP) observations. *Atmospheric Chem. Phys.* **18**, 5359–5370, DOI: 10.5194/acp-18-5359-2018 (2018).

84. van der Werf, G. R. *et al.* Global fire emissions estimates during 1997–2016. *Earth Syst. Sci. Data* **9**, 697–720, DOI: 10.5194/essd-9-697-2017 (2017).

Acknowledgements

We kindly acknowledge the provision of data from eddy-covariance sites (https://doi.org/10.18160/2G60-ZHAK) by Ivan Janssens, Annalea Lohila, Harry Lankreijer, Nicolas Delpierre, Luca Belelli Marchesini, Adriano Conte, Olli Peltola, Umberto Morra di Cella, Radek Czerný, Nina Buchmann, Pasi Kolari, Tarek Sebastian El-Madany, Clemens Drüe, Eric Dufrêne, Jiří Dušek, Maria Chiesa, Eeva-Stiina Tuittila, Ramon Lopez Jimenez, Frederik Schrader, Janne Levula, Shiva Ghiasi, Christophe Chipeaux, Corinna Rebmann, Frederik Uldall, Mika Korkiakoski, Juha-Pekka Tuovinen, Lenka Foltýnová, Henri Chopin, Eyal Rotenberg, Xuefei Li, Benoit Burban, Olaf Kolle, Frank Tiedemann, Laura Heimsch, Matthew Saunders, Risto Taipale, Luca Tezza, Ana Lopez Ballesteros, Louis Gourlez de la Motte, Antje Lucas-Moffat, Giuseppe de Simon, Manuel Acosta, Tanguy Manise, Johan Neirynck, Ladislav Sigut, Daniel Berveiller, Damien Bonal, Lutz Merbold, Benjamin Loubet, Tim De Meulder, Timo Vesala, Kim Pilegaard, Jean-Pierre Delorme, Lukas Siebicke, luca vitale, J. Thomas Gruenwald, Sigrid Dengel, Aurore Brut, Julia Kurbatova, Laura Dienstbach, Giovanni Manca, Thibaut Thyrion, Regine Maier, daniela famulari, Iris Feigenwinter, Liisa Kulmala, Marilyn Roland, Tiphaine Tallec, Riccardo Marzuoli, Mikael Ottosson Lofvenius, Sebastien Gogo, Petri Keronen, Alexander Graf, Barbara Marcolla, Nicola Arriga, Enrique P. Sanchez-Canete, Martin Hertel, Jutta Holst, Fatima Laggoun, Mana Gharun, Thomas Friborg, Kathrin Fuchs, Michal Heliasz, Edoardo Cremonese, Bernard Heinesch, Natalia Kowalska, Francisco Domingo Poveda, Silvano Fares, Tiziano Sorgi, Anne De Ligne, Denis Loustau, Jean-Christophe Calvet, Andreas Ibrom, Adrien Jacotot, Mats B. Nilsson, Caroline Vincke, Jan Segers, Meelis Mölder, Eric Ceschia, Ivan Mammarella, Martin Stecher, Sergio Aranda-Barranco, Paul di Tommasi, Guillaume Simioni, Dan Yakir, Andrea Pitacco, Bo Elberling, Anders Lindroth, Katerina Havrankova, Ganapati Sahoo, Giacomo Gerosa, Sebastian Gimper, Mika Aurela, Nadia Vendrame, Mirco Migliavacca, Eugenie Paul-Limoges, Angelo Finco, Andrew Kowalski, Oscar Perez-Priego, Markus Reichstein, Lukas Hörtnagl, Tuomas Laurila, Carmen Emmel, Arnaud Carrara, Werner Eugster, Daniel Dolfus, Pavel Alekseychik, Bernard Longdoz, Natalia Vygodskaya, Milan Fischer, Matteo Sottocornola, Fredrik Lagergren, Olivier Marloie, Ignacio Goded, Alexander Knohl, Christian Bruemmer, vincenzo Magliulo, Maria Rosario Moya Jimenez, Heikki Laakso, Leonardo Montagnani, Jonathan Muller, Pauline Buysse, Marta Galvagno, Damiano Gianelle, Matthias Cuntz, Penelope Serrano, Charlotte Sigsgaard, Franco Meggio, Christian Bernhofer, Per Marklund, Valerio Moretti, Efrat Schwartz, Marian Pavelka, Frederic Guibal, Marius Schmidt, Matthias Peichl, Andrej Varlagin, Anna Tedeschi, Rasmus Jensen, Eleonora Canfora, Carlo Trotta, Dario Papale.

As well as from atmospheric sites by Bergamaschi, P., Colomb, A., De Mazière, M., Emmenegger, L., Kubistin, D., Lehner, I., Lehtinen, K., Lund Myhre, C., Marek, M., Platt, S.M., Plaß-Dülmer, C., Schmidt, M., Apadula, F., Arnold, S., Blanc, P.-E., Brunner, D., Chen, H., Chmura, L., Conil, S., Couret, C., Cristofanelli, P., Delmotte, M., Forster, G., Frumau, A., Gheusi, F., Hammer, S., Haszpra, L., Heliasz, M., Henne, S., Hoheisel, A., Kneuer, T., Laurila, T., Leskinen, A., Leuenberger, M., Levin, I., Lindauer, M., Lopez, M., Lunder, C., Mammarella, I., Manca, G., Manning, A., Marklund, P., Martin, D., Meinhardt, F., Müller-Williams, J., Necki, J., O'Doherty, S., Ottosson-Löfvenius, M., Philippon, C., Piacentino, S., Pitt, J., Ramonet, M., Rivas-Soriano, P., Scheeren, B., Schumacher, M., Sha, M.K., Spain, G., Steinbacher, M., Sørensen, L.L., Vermeulen, A., Vítková, G., Xueref-Remy, I., di Sarra, A., Conen, F., Kazan, V., Roulet, Y.-A., Biermann, T., Heltai, D., Hensen, A., Hermansen, O., Komínková, K., Laurent, O., Levula, J., Pichon, J.-M., Smith, P., Stanley, K., and Trisolino, P., https://doi.org/10.18160/CEC4-CAGK

The measurements at WAO are funded by the UK's National Centre for Atmospheric Sciences (NCAS).
CO_2
observations at Jungfraujoch are supported by ICOS Switzerland (ICOS-CH) Phase 3 (Swiss National Science Foundation, grant 20F120_198227).

CH-Dav was supported by the SNF projects ICOS-CH Phase 1-3 (20FI21_148992, 143 20FI20_173691, 20F120_198227) and the EU project RINGO 730944.

We acknowledge Guido van der Werf for his help on the fire flux estimates and kindly thank Imme Benedict for providing the GPH data.

Author contributions statement

WP designed the study together with AB, SS, IL, and PC. AvdW, EJ, YX, and GK did the analyses. WP and AvdW wrote the manuscript with help from all co-authors. SL, BL, PHC, DL MR, TK, and DK provided observations shown in the manuscript. SB ran the STILT transport model. RK provided CTE-HR output. AB and SS provided OCN and JULES output data. PC provided fire estimates. All authors gave textual feedback on the manuscript.

Competing interests

The authors declare that they do not have any competing interests

Data and code availability

All data and code are available upon reasonable request. All SiB4 and GFAS fire fluxes used in this study are available at https://doi.org/10.18160/20Z1-AYJ2.

Supplementary Files

This is a list of supplementary files associated with this preprint. Click to download.

- Droughtmanuscriptsupplement.pdf